Substitution Effects and Linear Free Energy Relationships during Reduction of 4-Benzoyl-*N*-(4-substituted benzyl)pyridinium Cations

Nicholas Leventis[*,‡], Guohui Zhang[§], Abdel-Monem M. Rawashdeh[§] and Chariklia Sotiriou-Leventis[*,§]

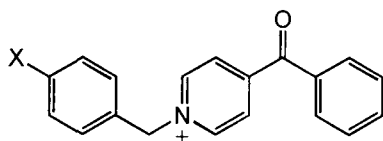[‡] Materials Division, NASA Glenn Research Center, 21000 Brookpark Road, M. S. 49-1, Cleveland, OH 44135

[§] Department of Chemistry, University of Missouri-Rolla, Rolla, MO 65409

Nicholas.Leventis@grc.nasa.gov and cslevent@umr.edu

tel.: (216) 433-3202 (N.L.); (573) 341-4353 (C. S.-L.)

ABSTRACT

In analogy to 4-(*p*-substituted benzoyl)-*N*-methylpyridinium cations (**1-X's**), the title species (**2-X's**, -X = -OCH$_3$, -CH$_3$, -H, -Br, -COCH$_3$, -NO$_2$) undergo two reversible, well-separated ($E_{1/2} \geq 650$ mV) one-electron reductions. The effect of substitution on the reduction potentials of **2-X's** is much weaker than the effect of the same substituents on **1-X's**: the Hammett ρ-values are 0.80 and 0.93 for the 1st- and 2nd-e reduction of **2-X's** vs. 2.3 and 3.3 for the same reductions of **1-X's**, respectively. Importantly, the nitro group of **2-NO$_2$** undergoes reduction before the 2nd-e reduction of the 4-benzoylpyridinium system. These results suggest that the redox potentials of the 4-benzoylpyridinium system can be course-tuned via *p*-benzoyl substitution and fine-tuned via *p*-benzyl substitution. Introducing the recently derived substituent constant of the –NO$_2^{\cdot-}$ group ($\sigma_{p-NO_2^-}$ = -0.97) yields an excellent correlation for the 3rd-e reduction of **2-NO$_2$** (corresponding to the reduction of the carbonyl group) with the 2nd-e reduction of the other **2-X's**, and confirms the electron donating properties of –NO$_2^{\cdot-}$.
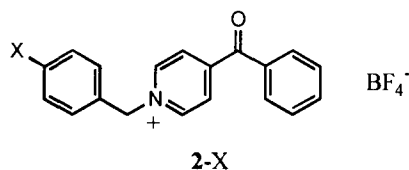
We reported recently that 4-benzoyl-N-methylpyridinium cations, 1-X's, undergo two successive, well-separated ($\sim$0.6 V) one-electron (1-e) reductions where the 1^{st}-e neutralizes the pyridinium and the 2^{nd} one yields the enolate, [1-X]$^-$ (eq 1).[1,2]
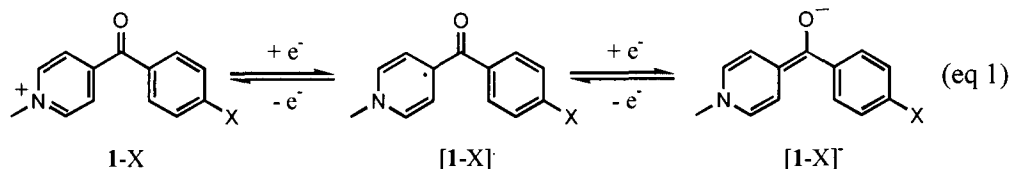
The 1-e reduced ketones [1-X]$^{\cdot}$ are stable towards pinacolization,[1] while the 2-e reduced forms [1-X]$^-$ (eq 1) are chemically stable only in the absence of proton donors. In the presence of protic acids [1-X]$^{\cdot}$'s develop hydrogen (H)-bonding through the enolate-O, shifting the second cyclic voltammetric reduction wave to more positive potentials; the first reduction wave remains completely unaffected.[1,2] H-bonded adducts with stronger acids (e.g., CH_3CO_2H) undergo irreversible proton transfer to the corresponding *quaternized* carbinols within the time scale (20-30 s) of cyclic voltammetry at 0.1 V s^{-1}.[1] H-bonded adducts with weak protic acids (e.g., water, alcohols) undergo proton transfer on longer time scales ($\sim$400 s) to the corresponding *non-quaternized* carbinols.[1] These findings suggest that this class of compounds could be used as main-stream redox catalysts or electron-transfer quenchers, while in aprotic environments they could be used as electrochromic materials (turning from colorless to red upon 1-e reduction), for which the basic requirement is chemical reversibility.[2] In view of those applications, the synthetic accessibility of the *para*-position of the benzoyl group provides an additional degree of freedom, by allowing tuning of the redox properties of the 4-benzoylpyridinium system (1-X) through the electronic properties of the substituent X (eq 1). As expected, both reductions are facilitated by electron-withdrawing substituents, and it was found experimentally that both $E_{1/2}$'s correlate well with the substituent constants, σ_{p-X}. In that context, the 2nd-e reduction is more sensitive to the electronic properties of the substituent (ρ_{2-e}=3.3) than the first one (ρ_{1-e}=2.3), reflecting the relative distance of the substituent from the point of reduction.[2] Along those studies, it was also observed that the nitro group of 1-NO$_2$ undergoes reduction before the carbonyl. So, when the carbonyl group of 1-NO$_2$ is reduced, -NO$_2$ has been already transformed into -NO$_2$$^{\cdot-}$. Reasoning that the redox potential of the carbonyl

reduction of **1-NO₂** (third wave) should correlate with the corresponding redox potentials of the other **1-X**'s (second waves), has allowed calculation of the substituent constant for $-NO_2^{\cdot-}$. It was found that $\sigma_{p-NO_2^{\cdot-}}$ = -0.97, suggesting that $-NO_2^{\cdot-}$ is a strong electron donor.[2]

Hammett Linear Free Energy correlations are used generally in order to quantify experimental observations and deduce stereoelectronic communication effects (e.g., resonance vs. inductive) between substituents and reaction sites. By the same token, Hammett correlation studies with compounds undergoing successive e-transfer reactions are rather uncommon.[3] So, motivated by the results summarized above, we decided to explore how reduction of the two redox centers would be affected by placing the substituents closer to the pyridinium rather than to the carbonyl, and thus perhaps get a glimpse of how the redox properties of the 4-benzoylpyridinium system could be adjusted by varying the two sets of substitutents independently. These issues were investigated with compounds **2-X**, where X= -OCH₃, -CH₃, -H, -Br, -COCH₃ and -NO₂.

2-X

All six **2-X**'s were prepared by straigthforward quaternization of 4-benzoylpyridine with the corresponding *p*-substituted benzyl halides. With the exception of the chloride salt of **2-H**, which was first reported in 1959 in conjunction with its potential properties as a local anesthetic,[4] all other **2-X**'s are new compounds.

Generally, the redox properties of **2-X**'s were determined with 3 mM solutions by cyclic voltammetry at 0.1 V s⁻¹ in anhydrous CH₃CN/0.1 M tetrabutylammonium perchlorate (TBAP) using ferrocene as internal standard. All electrochemical data are summarized in Table 1 and representative voltammograms are shown in Fig. 1. With the exception of **2-NO₂**, all other **2-X**'s show two chemically reversible redox waves (cathodic-to-anodic peak current ratios, $i_{p,c}/i_{p,a} \sim 1$). By analogy to **1-X**'s (eq 1), all first reduction waves correspond to the reduction of the pyridinium moieties, and with the exception of **2-NO₂**, all second reduction waves correspond to the reduction of the carbonyl. In most cases, the cathodic to anodic peak-to-peak potential separations, ΔE_{p-p},

are comparable to the values given by the ferrocenium/ferrocene (Fc^+/Fc) couple (73 ± 2 mV),[6] and are close to the theoretical value of 60 mV for 1-e kinetically reversible systems. As expected, Fig. 1A shows that electron-withdrawing substituents facilitate both reductions, as both waves move to less negative potentials. However, the effect of substitution does not appear to be strong. Meanwhile, the behavior of the nitro-derivative, $2\text{-}NO_2$, is remarkably different: at 0.1 V s^{-1} $2\text{-}NO_2$ shows four irreversible waves (Fig. 1B dotted line). A potential sweep at the same sweep rate through the first wave only shows that the 1st-e reduction of $2\text{-}NO_2$ is chemically reversible (see Table 1 and Fig. S.1 in Supporting Information). On the other hand, successive potential sweeps through the 2nd- and 3rd-e reduction waves of $2\text{-}NO_2$ produce irreversible behavior (see Fig.s S.2 and S.3 in Supporting Information). By decreasing the concentration of $2\text{-}NO_2$ to ~0.3 mM and by increasing simultaneously the sweep rate to ≥ 5 V s^{-1}, $2\text{-}NO_2$ yields three apparently reversible voltammetric waves (Fig. 1B solid line). The first wave correlates with the first reduction wave of all other $2\text{-}X$'s (*vide infra*) and corresponds to the reduction of the pyridinium ring (in analogy to eq 1); as expected, it is positively-shifted in comparison to the first waves of the other $2\text{-}X$'s (Table 1), reflecting the strong electron withdrawing properties of $-NO_2$. The second (middle) wave of $2\text{-}NO_2$ is close to the reduction of nitrobenzene (see Fig. 1B-inset), and is associated with the reduction of the *p*-nitrobenzyl substituent (eq 2). The third wave is due to the reduction of the

$$[2\text{-}NO_2] \quad \underset{-\text{ e}^-}{\overset{+\text{ e}^-}{\rightleftharpoons}} \quad [2\text{-}NO_2^{\cdot-}] \qquad \text{(eq 2)}$$
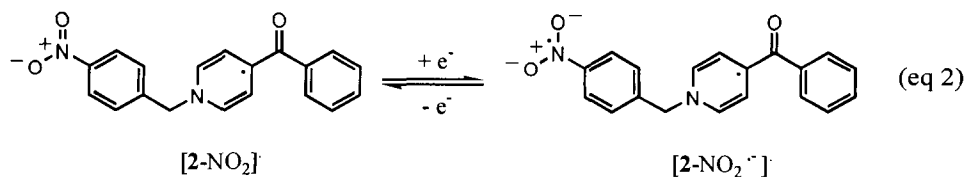
carbonyl and it has been shifted to more *negative* potentials, in contrast to the 2nd waves of all other $2\text{-}X$'s, which move in the positive direction as the electron-withdrawing ability of the substituents increases (Table 1). As it will be discussed below, this is attributed to the electron donating properties of $-NO_2^{\cdot-}$. Meanwhile, the fact that the three expected reversible waves are observed only by simultaneously decreasing the concentration of $2\text{-}NO_2$ and increasing the potential sweep rate, indicates that the 2-e reduced form, $[2\text{-}NO_2^-]^{\cdot-}$, participates in irreversible bimolecular reactions. This deduction, taken together with the fact that the 1-e reduced form of nitrobenzene does not

4

seem to interfere with the redox processes of **1-H** (Fig. 1B-inset), suggests that the reduced nitrobenzyl group is not involved, at least initially, in any bimolecular reaction. Therefore, it is suggested that the bimolecular reaction responsible for the irreversibility introduced as early as during the 0.1 V s^{-1} sweep through the second reduction wave of **2-NO$_2$**, should be related to the electrostatic perturbation imposed by $-NO_2^{-}$ upon the reduced pyridinium group of the same [**2-NO$_2^{-}$**]$^{\cdot}$ species.[7]

The relative efficiency by which substituents X influence the reduction of the two redox centers of the **2-X**'s is expressed via Hammett Linear Free Energy relationships. Fig. 2 shows good correlations between substituent constants σ_{p-X} and the $E_{1/2}$ of both waves of **2-X**'s. The slopes are 0.047 V and 0.055 V for the reduction of the pyridinium and the carbonyl, corresponding to reaction constants ρ_{1-e}=0.80 and ρ_{2-e}=0.93, respectively. It should be noted here that by using the σ_{p-NO_2} value (0.78), neither the second nor the third wave of **2-NO$_2$** correlate with the second waves (reduction of the carbonyl) of the other **2-X**'s. However, using the $\sigma_{p-NO_2^{-}}$ (= -0.97) value,[2] the reduction of the carbonyl group of **2-NO$_2$** (third voltammetric wave, Fig. 2B solid line), correlates well with the reduction of the same group in all other **2-X**'s. That finding confirms both the stereoelectronic communication between the *para*-benzyl substituents and the reduction sites, and the predictive power of the $\sigma_{p-NO_2^{-}}$ constant. Now, the good correlation of all $E_{1/2}$'s with the substituent constants σ_{p-X} indicates a purely inductive interaction, and the fact that ρ_{2-e} is somewhat larger than ρ_{1-e} was rather unexpected. On the other hand, both ρ-values are <1.00, reflecting a rather poor electronic communication of the substituents with the redox sites. (Note that ρ-values less than "one" are well established with thermodynamic parameters -equilibrium constants- in systems containing methylene spacers.[9]) The weak electronic communication of the substituents even with the point of the 2nd-e reduction (where the ρ-value is somewhat higher) is reflected upon the lack of any significant ability of the *p*-benzyl sustituents to affect H-bonding developing between the enolate oxygen and methanol in solution. In analogy to **1-X**'s, such H-bonding shifts the wave of the second electron reduction to more positive potentials leaving the first wave unaffected (Fig. 3). The slope of the potential separation between the two waves vs. log([MeOH]) (Fig. 3-inset) yields the

average (apparent) number of methanol molecules, $<m>$, participating in the H-bonded adducts, $[2\text{-}X]^-...m(CH_3OH)$ (see Table 2).[2] The intercepts of the same curves are related to the equilibrium constants (K_H), and therefore the free energy $(\Delta G^{o,f})$ of the H-bonded adduct formation.[1,2] While in the case of **1**-X's substitution played a significant role both on the strength of H-bonding and the number of MeOH molecules associating with the enolate-O, in the case of **2**-X's there is little variation in either one of those two properties as a function of substitution.

In conclusion, the effect of *para*-benzyl substituents on the reduction of the quaternized 4-benzoylpyridinium system is significantly weaker than the effect of *para*-benzoyl substitution. This finding implies that the redox potential of the 4-benzoylpyridinium system can be tuned first via *para*-benzoyl substitution and then fine-tuned via *para*-benzyl substitution. For example, based on our previous results with **1**-X's,[2] it is expected that a change of the *para*-benzoyl substituent from $-OCH_3$ to $-CH_3$ $(\Delta\sigma_{p-X} = 0.3)$ will change the redox potential of the 1st-e reduction of the 4-benzoyl-*N*-benzylpyridinium system by ~40 mV. Then a change of the *para*-benzyl substituent from $-OCH_3$ to $-NO_2$ $(\Delta\sigma_{p-X} = 1.05)$ is expected to change the redox potential of the same reduction by ~50 mV, and therefore by judicious choice of the *para*-benzyl substituents the potential range between the 1st-e reductions of the 4-(p-CH$_3$O-benzoyl)- and the 4-(p-CH$_3$-benzoyl)-*N*-benzylpyridinium cations can be covered almost continuously.

Supporting Information Available: (a) Experimental section with preparation and characterization of **2**-X's. (b) Cyclic voltammetry of **2**-NO$_2$ at 0.1 V s^{-1} through the first only (Fig. 1.S), the second (Fig. 2.S) and the first three (Fig. 3.S) reduction waves.

Table 1. Data for the reduction of **2-X**'s and of nitrobenzene (PhNO$_2$), in CH$_3$CN/0.1 M TBAP. [a]

2-X	$\sigma_{p\text{-}X}$ [b]	$E_{1/2}(1)$ V	$\Delta E_{p\text{-}p}(1)$ mV	$i_{p,c}/i_{p,a}(1)$	$E_{1/2}(2)$ V	$\Delta E_{p\text{-}p}(2)$ mV	$i_{p,c}/i_{p,a}(2)$	$E_{1/2}(3)$ V	$\Delta E_{p\text{-}p}(3)$ mV	$i_{p,c}/i_{p,a}(3)$
2-OCH$_3$	-0.27	-1.037 ± 0.001	73 ± 1	1.00	-1.698 ± 0.001	76 ± 1	1.04	—	—	—
2-CH$_3$	-0.14	-1.034 ± 0.002	66 ± 3	1.02	-1.682 ± 0.003	72 ± 5	1.06	—	—	—
2-H	0.00	-1.020 ± 0.002	68 ± 3	1.04	-1.691 ± 0.003	70 ± 3	1.06	—	—	—
2-Br	0.26	-1.009 ± 0.001	72 ± 2	1.03	-1.651 ± 0.001	75 ± 2	1.01	—	—	—
2-COCH$_3$	0.47	-1.003 ± 0.001	69 ± 4	1.09	-1.654 ± 0.001	75 ± 4	1.07	—	—	—
2-NO$_2$	0.78	-0.988 ± 0.003 [c]	74 ± 2 [c]	0.99	-1.499 ± 0.001 [d]	99 ± 3 [d]	e	-1.728 ± 0.002 [d]	135 ± 4 [d]	e
Ph-NO$_2$		-1.548 ± 0.003	73 ± 1	1.00						

[a]   With the exception of **2**-NO$_2$ (see footnote d), all $E_{1/2}$'s were determined by cyclic voltammetry at 0.1 V s^{-1} with ~3 mM solutions of the **2-X**'s, and are reported vs. the ferrocenium/ferrocene couple used as internal standard.

[b]   From ref. 5.

[c]   Determined with a 3 mM solution and a 0.1 V s^{-1} sweep rate.

[d]   Determined with a ~0.3 mM solution and a 5 V s^{-1} sweep rate.

[e]   Merging waves; baseline current could not be established (see Fig. 1B).

7

Table 2. Slopes, intercepts and other data related to the H-bonded adducts $[2\text{-}X]^-\ldots m(CH_3OH)$ derived from the plots of $\Delta E_{1/2}$ vs. $\log[CH_3OH]$ (see Fig. 3 - inset).[a]

$[2\text{-}X]^-$	$\sigma_{p\text{-}X}$	$d\Delta E_{1/2}/d \log$ [methanol][b]	$\langle m \rangle$[c]	Intercept[b]	r^2	$K_H \times 10^{-3}$[d]	$\Delta G^{\circ,f}$[e]
$[1\text{-}NO_2{}^{\cdot}]^-$	-0.97	144	2.43 (2)	-542	0.993	2.27	-4.57
$[1\text{-}OCH_3]^-$	-0.27	134	2.27 (2)	-441	0.978	5.36	-5.08
$[1\text{-}CH_3]^-$	-0.14	140	2.37 (2)	-448	0.983	2.45	-4.62
$[1\text{-}H]^-$	0.00	139	2.35 (2)	-455	0.985	4.58	-4.99
$[1\text{-}Br]^-$	0.26	135	2.28 (2)	-439	0.976	2.76	-4.69
$[1\text{-}COCH_3]^-$	0.47	128	2.16 (2)	-453	0.983	2.27	-4.57

[a] $\Delta E_{1/2} = E_{1/2}(2) - E_{1/2}(1)$. $\Delta E_{1/2}$ reports the position of the second wave, $E_{1/2}(2)$, with respect to the fixed position of the first one, $E_{1/2}(1)$.

[b] in mV.

[c] $\langle m \rangle$ = slope of the $\Delta E_{1/2}$ vs. $\log[CH_3OH]$ curve (see Fig. 3 Inset) divided by 59.16 mV;[2] in parentheses are first significant figure approximations for the average (apparent) number of CH_3OH molecules participating in the H-bonded adducts.

[d] in M^{-m}.

[e] in kcal/mol.

References

1. Leventis, N.; Elder, I. A.; Gao, X.; Bohannan, E. W.; Sotiriou-Leventis, C.; Rawashdeh, A.-M. M.; Overschmidt, T. J.; Gaston, K. R. *J. Phys. Chem. B* **2001**, *105*, 3663-3674.

2. Leventis, N.; Rawashdeh, A.-M. M.; Zhang, G.; Elder, I. A.; Sotiriou-Leventis, C. *J. Org. Chem.* **2002**, *67*, 7501-7510.

3. See for example: (a) Sauro, V. A.; Workentin, M. S. *J. Org. Chem.* **2001**, *66*, 831-838. (b) Connelly, N. G.; Davis, P. R. G.; Harry, E. E.; Klangsinsirikul, P.; Venter, M. *J. Chem. Soc., Dalton Trans.* **2000**, 2273-2277. (c) Zagal, J. H.; Gulppi, M. A.; Cardenas-Jiron, G. *Polyherdon* **2000**, *22-23*, 2255-2260. (d) Aguilar-Martinez, M.; Cuevas, G.; Jimerez-Estrada, M.; Gonzalez, I.; Lotina-Hennsen, B.; Macias-Ruvalcaba, N. *J. Org. Chem.* **1999**, *64*, 3684-3694. (e) McInnes, E. J. L.; Farley, R. D.; Rowlands, C. C.; Welch, A. J.; Rovatti, L.; Yellowlees, L. J. *J. Chem. Soc., Dalton Trans.*, **1999**, 4203-4208. (f) Andersen, M. L.; Nielsen, M. F.; Hammerrich, O. *Acta Chem. Scand.* **1997**, *51*, 94-107. (g) Darensbourg, M. Y.; Bischoff, C. J.; Houliston, S. A.; Pala, M.; Reibenspies, J. *J. Am. Chem. Soc.* **1990**, *112*, 6905-6912.; (h) Queiros, M. A. M.; Simao, J. E. J.; Dias, A. R. *J. Organomet. Chem.* **1987**, *329*, 85-97.

4. Lyle, R. E.; Troscianiec, H. J.; Warner, G. H. *J. Org. Chem.* **1959**, *24*, 338-42.

5. Isaacs, N. Physical Organic Chemistry, 2nd ed.; Longman Scientific and Technical: Essex, U.K., 1995: p 152.

6. Daschbach, J.; Blackwood, D.; Pons, J. W.; Pons, S. *J. Electroanal. Chem.* **1987**, *237*, 269-273.

7. Once the $-NO_2$ group is reduced to the strongly electron donating $-NO_2{}^{\cdot-}$ group, the reduced pyridinium group of the same species becomes a reducing agent for the pyridinium of **2-NO₂**. So, [**2-NO₂⁻**]⁻ diffusing away from the electrode can react in a comproportionation fashion with **2-NO₂** diffusing towards the electrode and yield not only 2 moles of [**2-NO₂**]⁻, but also [**2-NO₂⁻**]⁻.[8] The latter is a new species that is generated only transiently because, upon reduction, the $-NO_2$ group changes from an electron acceptor into an electron donor. [**2-NO₂⁻**] finds itself in two concentration gradients, one towards the electrode and one towards the bulk solution. [**2-NO₂⁻**] diffusing towards the electrode is reduced into [**2-NO₂⁻**]⁻. [**2-NO₂⁻**]⁻ lost by diffusion towards the bulk becomes responsible for the chemical irreversibility observed past the second wave.

8. (a) Leventis, N.; Gao, X. *J. Electroanal. Chem.* **2001**, *500*, 78. (b) Rongfeng, Z.;
Evans, D. H. *J. Electroanal. Chem.* **1995**, *385*, 201.

9. For example, the ρ values for the ionization (in water) of $ArCO_2H$, $ArCH_2CO_2H$ and $ArCH_2CH_2CO_2H$ are 1.00, 0.56 and 0.24 respectively (Ar: substituted phenyl group).[10]

10. Carey, F. A.; Sundberg, R. J. Advanced Organic Chemistry, Third Edition, Part A: Structure and Mechanisms; Plenum Press: New York, N.Y., 1993: p 202.

Figure Captions

Figure 1. (A) Cyclic Voltammetry of **2-OCH$_3$** (- - - - ; 3.04 mM), **2-H** (———; 3.32 mM, and **2-COCH$_3$** (. . . . ; 3.27 mM) in CH$_3$CN/0.1 M TBAP with a Au-disk electrode (0.0201 cm^2) at 0.1 V s^{-1}. Current bar: 10 µA (B) Cyclic Voltammetry of **2-NO$_2$** 0.33 mM at 0.1 V s^{-1} (. . . . . ; current bar: 2.7 µA) and at 5 V s^{-1} (———; current bar: 16 µA). Inset: Voltammetry in the same electrolytic solution at 0.1 V s^{-1} of a mixture containing **1-H** (3.08 mM) and nitrobenzene (PhNO$_2$, 1.90 mM). The middle wave is produced by the reduction of PhNO$_2$. Similar results have been obtained with **2-H** and PhNO$_2$.

Figure 2. Hammett plots for the 1st-e reduction (dark circles; slope = 0.047 V; intercept = -1.023 V; correlation (r^2) =0.981) and the 2nd-e reduction (open circles; slope = 0.055 V; intercept = -1.678 V; correlation (r^2) = 0.908) for the 4-benzoyl-N-(p-substituted benzyl)pyridinium cations (**2-X**'s) of Table 1. The open triangle corresponds to the 1-e reduction of the p-nitrobenzyl moiety of **2-NO$_2$** (refer to the middle wave in Figure 1B).

Figure 3. The effect of methanol on the cyclic voltammetry of **2-CH$_3$** (3.44 mM) in CH$_3$CN/0.1 M TBAP at 0.1 V s^{-1}, using a Au-disk electrode (0.0201 cm^2). [CH$_3$OH[: (a) 0.0 M; (b) 0.098 M; (c) 0.196 M; (d) 0.484 M; (e) 0.95 M; (f) 2.24 M. Inset: $|\Delta E_{1/2}|$ of the two waves vs. log[CH$_3$OH]; slope = 140 mV; intercept = 448 mV; correlation (r^2) = 0.983.
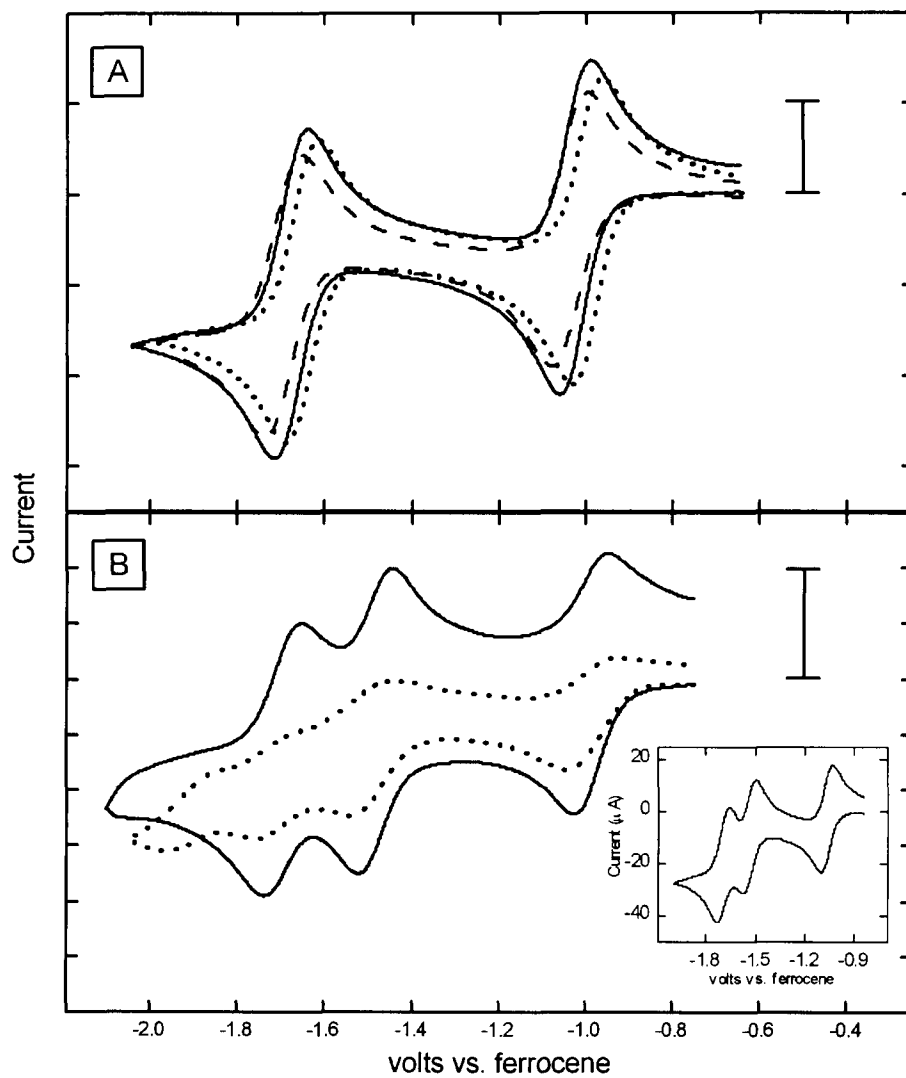
Figure 1

Current

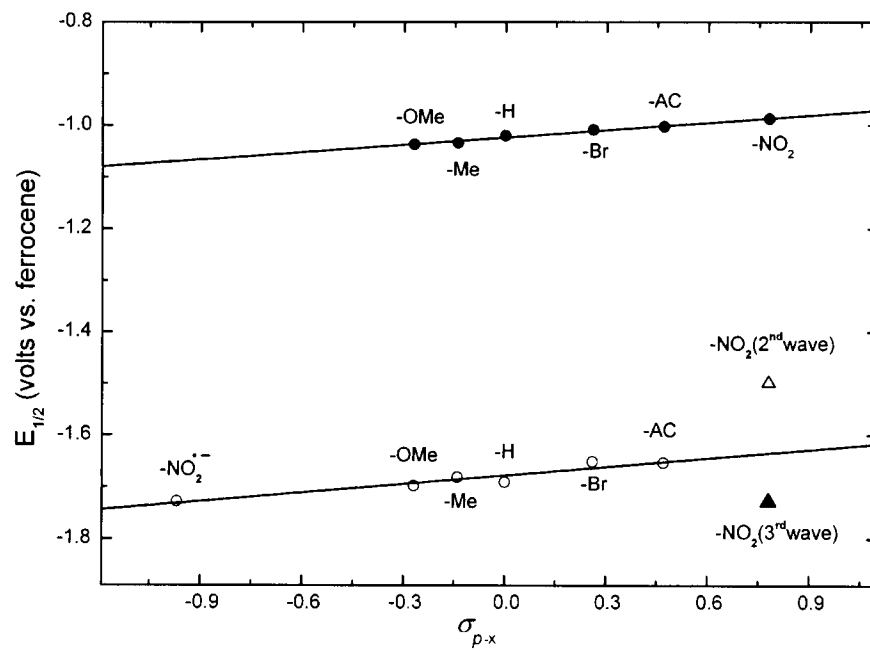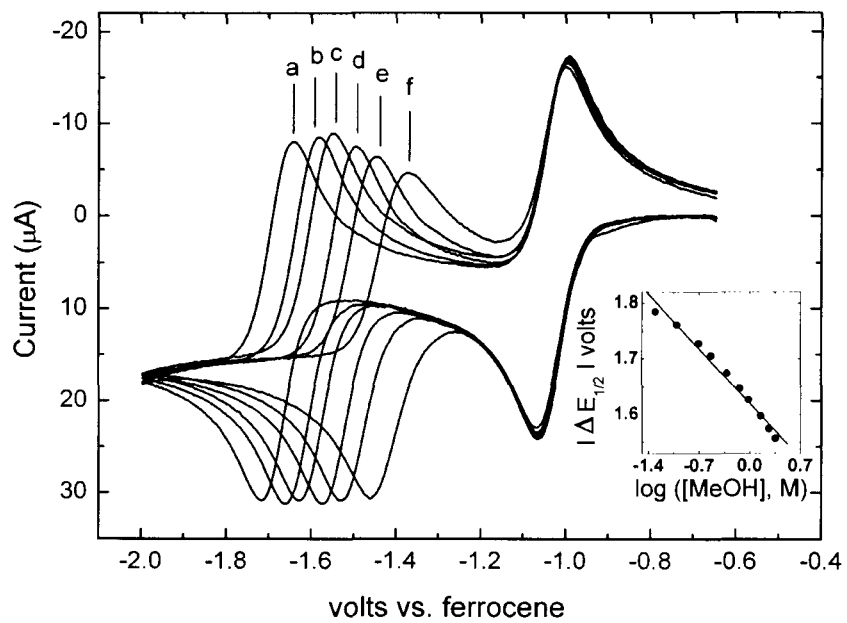volts vs. ferrocene

Figure 2

Figure 3

Substitution Effects and Linear Free Energy Relationships during Reduction of 4-Benzoyl-*N*-(4-substituted benzyl)pyridinium Cations

Nicholas Leventis[*,‡], Guohui Zhang[§], Abdel-Monem M. Rawashdeh[§] and Chariklia Sotiriou-Leventis[*,§]

[‡] Materials Division, NASA Glenn Research Center, 21000 Brookpark Road, M. S. 49-1, Cleveland, OH 44135

[§] Department of Chemistry, University of Missouri-Rolla, Rolla, MO 65409

Nicholas.Leventis@grc.nasa.gov and cslevent@umr.edu

SUPPORTING INFORMATION

Experimental Section

Methods. All electrochemical experiments were carried out with an Au disk working electrode (1.6 mm in diameter, from Bioanalytical Systems, Inc., West Lafayette, IN), an aqueous Ag/AgCl reference electrode (also from BAS), and an Au foil (2.5 cm^2) as a counter electrode, in Ar-degassed anhydrous CH_3CN/0.1 M TBAP solutions at room temperature (23 ±1 °C). All voltammograms have been 80% compensated for solution resistance. All reactions were carried out under N_2. Melting points are uncorrected. Elemental analyses were performed by Prevalere Life Sciences, Inc. (Former Oneida Research Services, Inc.), Whiteboro, NY.

Materials. All starting materials, reagents and solvents were commercially available and were used as received. Ferrocene and 4-benzoylpyridine were sublimed. Tertrabutylammonium perchlorate (TBAP) was prepared as described before.[1] All **2-X**'s were prepared by quaternization of 4-benzoylpyridine according to the following general procedure. 4-Benzoylpyridine (1 equiv) and the corresponding *p*-substituted benzyl halide (2-3 equiv bromide or chloride) were dissolved in CH_3CN and refluxed for 24 h. At the end of the period, the solvent was removed and the

[1] Leventis, N.; Elder, I. A.; Gao, X.; Bohannan, E. W.; Sotiriou-Leventis, C.; Rawashdeh, A.-M. M.; Overschmidt, T. J.; Gaston, K. R. *J. Phys. Chem. B* **2001**, *105*, 3663.

residue was dissolved in water. An aqueous solution of ammonium tertrafuoroborate (~10 equiv) was added and the mixture was refluxed until all solids were dissolved. The solution was cooled to ~ 5 °C, and the precipitate was collected, dissolved in CH_3CN and precipitated with diethylether. The precipitate was collected and recrystallized once again from water. All **2**-X's of this study are white solids. ^1H NMR assignments are based on the following numbering convention:

2-X

4-Benzoyl-*N*-benzylpyridinium tetrafluoroborate (**2**-H) was prepared from 4-benzoylpyridine (5g, 0.027mol) and benzyl bromide (14g, 0.081mol). Yield 5.2 g (53%); mp 151-153°C; ^1H NMR (DMSO-d_6, 400 MHz) δ 5.93(2H, s, -CH_2N^+), 7.45-7.50 (3H, m, H-1,2,6), 7.58-7.63 (4H, m, H-3,5,17,19), 7.77-7.81 (1H, m, H-18), 7.83-7.86 (2H, m, H-16,20), 8.38 (2H, d, $J_{9,10} = J_{12,13} = 6.6$ Hz, H-9,13), 9.36 (2H, d, $J_{9,10} = J_{12,13} = 6.8$ Hz,, H-10,12); ^{13}C NMR (DMSO-d_6, 100 MHz) δ 63.5 (-CH_2N^+), 127.5, 129.2, 129.4, 129.6, 130.4, 133.9, 134.2, 134.9, 145.8, 151.9, 192.1 (C=O). Anal Calcd for $C_{19}H_{16}NOBF_4$: C, 63.19; H, 4.47; N, 3.88. Found: C, 62.92; H, 4.12; N, 3.91.

4-Benzoyl-*N*-(4-methylbenzyl)pyridinium tetrafluoroborate (**2**-CH$_3$) was prepared from 4-benzoylpyridine (5g, 0.027mol) and 4-methylbenzyl bromide (10g, 0.054mol). Yield 4.6 g (45%); mp 190-192°C; ^1H NMR (DMSO-d_6, 400 MHz) δ 2.32 (3H, s, -CH_3) 5.88 (2H, s, -CH_2N^+), 7.29 (2H, d, $J_{2,3}=J_{5,6}=8.0$ Hz, H-2,6), 7.50 (2H, d, $J_{2,3}=J_{5,6}=8.0$ Hz, H-3,5), 7.59-7.66 (2H, m, H-17,19), 7.77-7.82 (1H, m, H-18), 7.83-7.86 (2H, m, H-16,20), 8.37 (2H, d, $J_{9,10} = J_{12,13} = 6.8$ Hz, H-9,13), 9.34 (2H, d, $J_{9,10} = J_{12,13} = 6.8$ Hz, H-10,12); ^{13}C NMR (DMSO-d_6, 100 MHz) δ 20.8 (-CH_3), 63.5 (-CH_2N^+), 127.5, 129.0, 129.2, 129.7, 130.0, 130.4, 130.9, 134.1, 139.3, 145.6, 151.8, 192.1 (C=O). Anal Calcd for $C_{20}H_{18}NOBF_4$: C, 64.03; H, 4.84; N, 3.73. Found: C, 63.95; H, 4.55; N, 3.80.

4-Benzoyl-*N*-(4-nitrobenzyl)pyridinium tetrafluoroborate (**2**-NO$_2$) was prepared from 4-benzoylpyridine (5g, 0.027mol) and 4-nitro-benzyl bromide (10g,

0.047mol). Yield 7.8 g (71%); mp 145-147°C; ^{1}H NMR (DMSO-d_6, 400 MHz) δ 6.09 (2H, s, -CH$_2$N$^+$), 7.58-7.64 (2H, m, H-17,19), 7.70 (2H, d, $J_{2,3}$ = $J_{5,6}$= 9.0 Hz, H-3,5), 7.75-7.80 (1H, m, H-18), 7.82-7.85 (2H, m, H-20,26), 8.22 (2H, d, $J_{9,10}$ = $J_{12,13}$= 6.6 Hz, H-10,12), 8.30 (2H, d, $J_{2,3}$ = $J_{5,6}$= 8.8 Hz, H-2,6), 8.93 (2H, d, $J_{9,10}$ = $J_{12,13}$= 6.8 Hz, H-9,13); ^{13}C NMR (CD$_3$CN, 100 MHz) δ 64.4 (-CH$_2$N$^+$), 125.3, 128.9, 130.1, 131.3, 131.6, 135.2, 135.9, 140.3, 146.9, 149.8, 153.9, 192.1 (C=O). Anal Calcd for C$_{19}$H$_{15}$N$_2$O$_3$BF$_4$: C, 56.19; H, 3.72; N, 6.90. Found: C, 56.25; H, 3.36; N, 6.84.

4-Benzoyl-*N*-(4-methoxylbenzyl)pyridinium tetrafluoroborate (2-OCH$_3$) was prepared from 4-benzoylpyridine (5g, 0.027mol) and 4-methoxylbenzyl chloride (9g, 0.058mol). Yield 3.3 g (31%); mp 130-132°C; ^{1}H NMR (DMSO-d_6, 400 MHz) δ 3.77 (3H, s, -OCH$_3$), 5.85 (2H, s, -CH$_2$N$^+$), 7.03 (2H, d, $J_{2,3}$=$J_{5,6}$=8.8 Hz, H-3,5), 7.59 (2H, d, $J_{2,3}$=$J_{5,6}$=8.6 Hz, H-2,6), 7.61-7.65 (2H, m, H-17,19), 7.77-7.82 (1H, m, H-18), 7.83-7.86 (2H, m, H-16,20), 8.36 (2H, d, $J_{9,10}$ = $J_{12,13}$= 6.8 Hz, H-9,13), 9.34 (2H, d, $J_{9,10}$ = $J_{12,13}$= 7.0 Hz, H-10,12); ^{13}C NMR (DMSO-d_6, 100 MHz) δ 55.3 (-OCH$_3$), 63.3 (-CH$_2$N$^+$), 114.7, 125.7, 127.4, 129.1, 130.4, 131.0, 134.1, 134.8, 145.5, 151.7, 160.2, 192.1 (C=O). Anal Calcd for C$_{20}$H$_{18}$NO$_2$BF$_4$: C, 61.41; H, 4.64; N, 3.58. Found: C, 61.10; H, 3.94; N, 3.68.

4-Benzoyl-*N*-(4-bromobenzyl)pyridinium tetrafluoroborate (2-Br) was prepared from 4-benzoylpyridine (5g, 0.027mol) and 4-bromobenzyl bromide (12g, 0.049mol). Yield 5.9 g (51%); mp 188-190°C; ^{1}H NMR (DMSO-d_6, 400 MHz) δ 5.90 (2H, s, -CH$_2$N$^+$), 7.58 (2H, d, $J_{2,3}$=$J_{5,6}$=8.6 Hz, H-3,4), 7.59-7.65 (2H, m, H-16,20), 7.70 (2H, d, $J_{2,3}$-$J_{5,6}$=8.6 Hz, H-2,6), 7.77-7.82 (1H, m, H-18), 7.83-7.87 (2H, m, H-16,20), 8.38 (2H, d, $J_{9,10}$ = $J_{12,13}$= 6.8 Hz, H-9,13), 9.35 (2H, d, $J_{9,10}$ = $J_{12,13}$= 7.0 Hz, H-10,12); ^{13}C NMR (DMSO-d_6, 100 MHz) δ 62.8 (-CH$_2$N$^+$), 127.5, 129.2, 130.4, 132.2, 133.2, 134.2, 134.9, 145.8, 151.9, 192.1 (C=O). Anal Calcd for C$_{19}$H$_{15}$NOBrBF$_4$: C, 51.86; H, 3.44; N, 3.18. Found: C, 51.80; H, 2.55; N, 3.18.

**4-Benzoyl-*N*-(4-acetylbenzyl)pyridinium tetrafluoroborate (2-COCH$_3$)** was prepared from 4-benzoylpyridine (5g, 0.027mol) and 4-bromomethylacetophenone. The latter was prepared from 4-methylacetophenone (10g, 0.075mol), *N*-bromosuccinimide (15g, 0.084mol) and 1,1-azobis(cyclohexanecarbonitrile) (3.6g, 0.015mol) in 150 ml CCl$_4$ (reflux, 24 h) and was used as received (light yellow solid), without further purification. Yield 7.6 g (70%); mp 175-177°C; ^{1}H NMR (DMSO-d_6,

400 MHz) δ 2.59 (3H, s, -COCH$_3$) 6.02 (2H, s, -CH$_2$N$^+$), 7.60-7.65 (2H, m, H-17,19), 7.72 (2H, d, $J_{2,3}$=$J_{5,6}$=8.6 Hz, H-3,5), 7.77-7.83 (1H, m, H-18), 7.84-7.88 (2H, m, H-16,20), 8.04 (2H, d, $J_{2,3}$=$J_{5,6}$=8.6 Hz, H-2,6), 8.41 (2H, d, $J_{9,10}$ = $J_{12,13}$= 6.8 Hz, H-9,13), 9.39 (2H, d, $J_{9,10}$ = $J_{12,13}$= 7.0 Hz, H-10,12); ^{13}C NMR (DMSO-d_6, 100 MHz) δ 26.9 (-CH$_3$) 63.0 (-CH$_2$N$^+$), 127.5, 129.0, 129.3, 129.3, 130.4, 134.1, 134.9, 137.4, 138.6, 146.0, 152.0, 192.1 (C=O), 197.7 (acetyl C=O). Anal Calcd for C$_{21}$H$_{18}$NO$_2$BF$_4$: C, 62.56; H, 4.50; N, 3.47. Found: C, 62.47; H, 3.78; N, 3.50.

Figure S.1 Cyclic Voltammogram across the first reduction wave of **2**-NO$_2$ (~0.6 mM) in CH$_3$CN/0.1 M TBAP at 0.1 V s^{-1}.
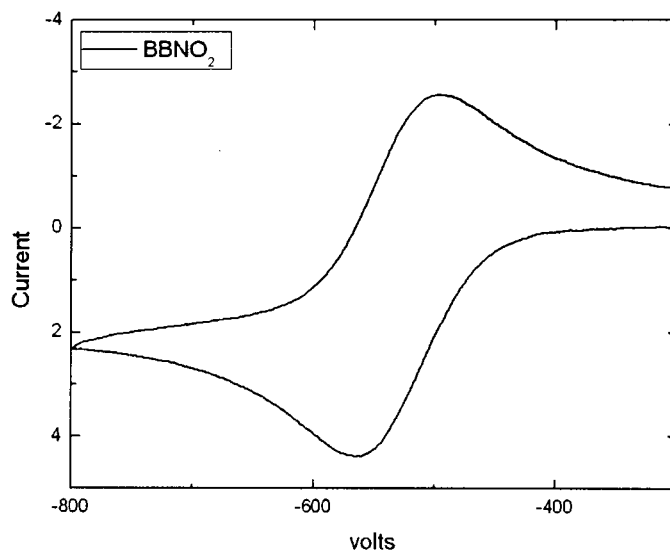
Figure S.2 Cyclic Voltammogram across the first two reduction waves of **2**-NO$_2$ (~0.6 mM) in CH$_3$CN/0.1 M TBAP at 0.1 V s^{-1}.
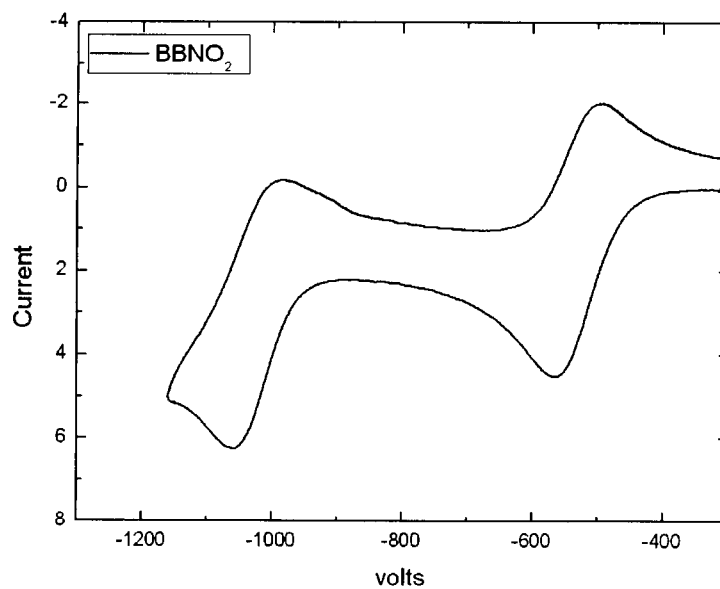
Figure S.3 Cyclic Voltammogram across the first three reduction waves of **2**-NO_2 (~0.6 mM) in CH_3CN/0.1 M TBAP at 0.1 V s^{-1}.